湖南沃溪钨-锑-金矿床的矿石组构学特征及其成因意义[*]

顾雪祥[1]   Oskar Schulz[2]   Franz Vavtar[2]   刘建明[3]   郑明华[4]

(1 中国科学院地球化学研究所，贵州 贵阳 550002；2 Institute of Mineralogy and Petrography, University of Innsbruck, A-6020 Innsbruck, Austria；3 中国科学院地质与地球物理研究所，北京 100101；4 成都理工大学，四川 成都 610059)

摘 要   通过对湖南沃溪矿床的宏观至微观尺度上的矿石组构学研究，揭示出矿床系同生热水沉积成因。层状矿体、细脉状矿化以及围岩蚀变之间的空间关系，指示了矿石与其所赋存的围岩同时形成。矿床形成后的变质-变形作用，主要使矿物发生重结晶、碎裂、位错以及小范围的再活化等。

关键词   地质学   矿石组构   沉积喷流   同生成因   钨锑金矿床   沃溪   湖南

中图分类号：P613.3；P618.67；P618.66；P618.51；P611   文献标识码：A

湖南沃溪矿床是扬子地台南缘江南元古代造山带内产出的为数众多的 W-Sb-Au 建造矿床的典型代表。长期以来，该矿床以其独特的白钨矿-辉锑矿-自然金密切共生的矿物组合，产于浅变质沉积岩系中完美的整合层状矿化以及显著的层控性，吸引了众多中外学者浓厚的研究兴趣。但迄今为止，有关该矿床的成因仍众说纷纭，莫衷一是，概括起来有岩浆热液成因(徐克勤，1965；张振儒，1980；1989；毛景文等，1997)、变质热液成因(罗献林等，1984；1996)、变质水和大气降水混合热液成因(杨燮，1992；牛贺才等，1992；刘英俊等，1993)、沉积-变质(改造)成因(朱炎龄等，1981；梁金城等，1981；肖启明等，1984；涂光炽等，1984；1987；梁博益等，1986；1988；李键炎，1989；鲍振襄，1989；1990；鲍振襄等，1991)、同生沉积成因(孟宪民等，1965)或海底喷气(热泉)沉积成因(张理刚，1985；1995)、层控-构造动力再造成因(刘亚军，1992a；1992b；1993；彭渤，1992)等观点。

近年来，笔者对湘西地区以沃溪为代表的产于元古界浅变质碎屑岩系地层中的钨-锑-金矿床开展了系统的岩石学、矿物学、组构学及地球化学研究(Gu et al.，2002a；2002b；2002c；Schulz et al.，

2001)。各种证据一致表明，沃溪矿床系晚元古代大陆地壳边缘弧后拉张环境下(Gu et al.，2002a)同生热水沉积作用的产物。本文仅从沃溪矿床的矿物学和组构学特征出发，探讨矿床的成因。有关该矿床的地球化学特征及所反映的成因信息，将另文论述。

1   矿床地质概况

矿床位于扬子地台南缘江南元古代造山带西段雪峰山弧形隆起带中段向北西凸出的转折部位。矿区位于轴向近东西的仙鹅抱蛋穹隆状背斜的北东翼，区内出露的地层自下而上有中元古界冷家溪群($Pt_2 lj$)、新元古界板溪群($Pt_3 bx$)以及上白垩统(K_2)陆相红色砂砾岩(图 1a)。其中，板溪群马底驿组($Pt_3 m$)和五强溪组($Pt_3 w$)是矿区内出露的主要地层，两者以横贯全区的沃溪逆断层为界，以北为五强溪组，以南为马底驿组。迄今所发现的矿体均位于断层以南马底驿组地层的中上部。矿区自西向东划分为红岩溪、鱼儿山、栗家溪、十六棚公和上沃溪 5个矿段。
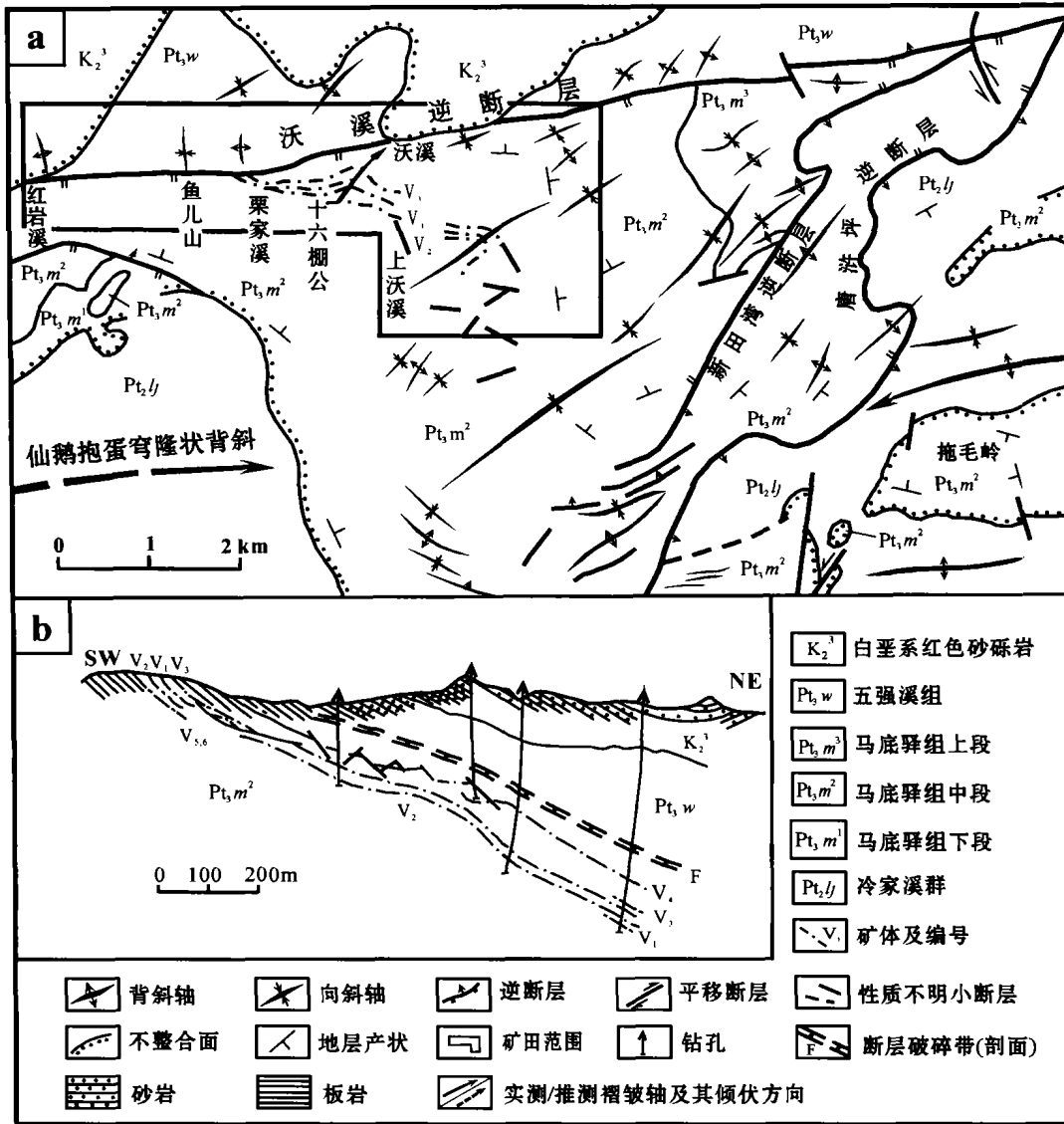
作为矿体直接围岩的马底驿组地层为一套浅

图 1　沃溪矿田及邻区地质-构造略图(a)及沃溪矿床 NE-SW 向典型剖面图(b)(据罗献林等，1996 修编)

Fig. 1　Sketch map showing geological-structural features of the Woxi ore field and its adjacent areas (a) and typical NE-SW section of the Woxi deposit (modified from Luo et al. , 1996)

变质（绿片岩相）的浊积岩（Gu et al. , 2002a, 2002b），依岩性变化可将其划分为 3 个岩性段：下段（$Pt_3 m^1$）厚 70～250 m，为灰绿色中至厚层浅变质石英砂岩和砂质板岩，底部与冷家溪群不整合接触面上常见一层厚度可达 1.5 m 的砾岩；中段（$Pt_3 m^2$）为主要的含矿层位，厚度变化大，从数十米至 800 m 不等，岩性为紫红色、灰紫色、紫灰色绢云母板岩，局部夹厚 0.1～10 m 的白云质灰岩透镜体。本段中上部靠近矿化层位含厘米级大小的具同心环带构造的钙质结核，结核中有时含浸染状白钨矿。上段（$Pt_3 m^3$）为厚 40～210 m 的灰绿色绢云母板岩和石英砂岩，局部夹紫红色板岩。

根据矿体产状、矿物组成和结构特征的差异以及与围岩相互关系的不同，矿化分为层状和脉状-网脉状两种主要类型。层状矿化占沃溪矿床总储量的 70％以上，由至少 9 个与地层产状严格整合的层状矿体（V_1～V_9）组成（V_1～V_6 见于图 1b、图 2、图 3a）。其中，位于层状矿化系统中部的 V_1～V_4 为主要的工业矿体，而 V_5～V_9 矿体规模较小、连续性较差，因而工业价值不大。矿层走向近东西，倾向北，倾角平缓（20～30°）。单个矿层的厚度（0.2～1.5 m）不大，但沿走向延长（40～350 m）和倾向延伸（通常300～
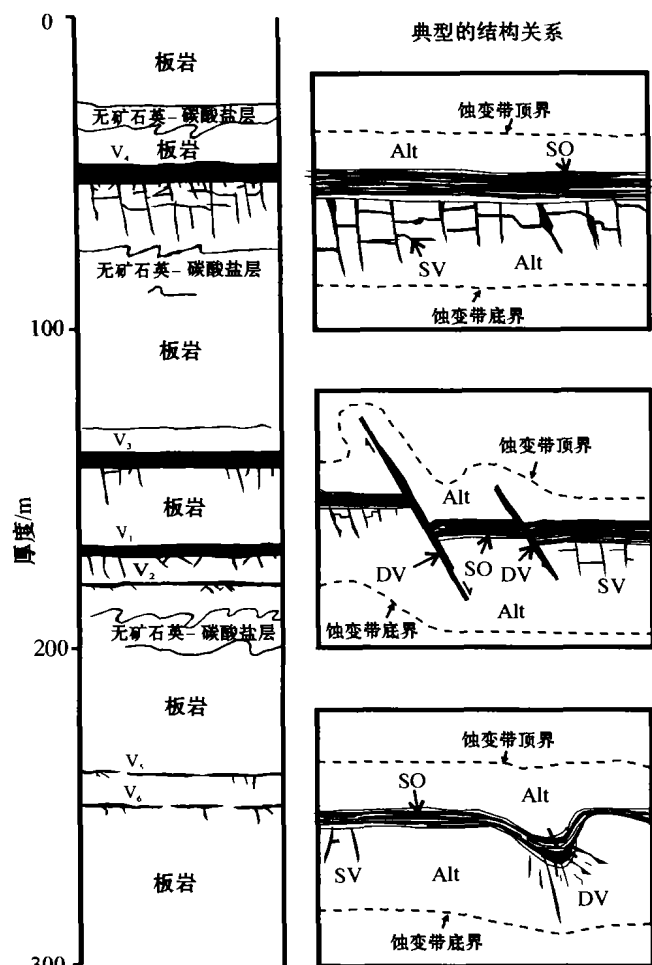
图 2　V_1-V_6 矿体在赋矿地层中的产出位置以及层状矿石（SO）、细脉状矿化（SV）、切层脉体（DV）和围岩蚀变（Alt）之间结构关系示意图

Fig. 2　Generalized stratigraphic section showing the location of orebodies V_1-V_6 and typical textural relations between stratiform ores (SO), stringers (SV), discordant veins (DV), and alteration blankets (Alt)

3500 m)远且稳定。矿石主要由韵律互层的条带状和（或）层纹状含金石英、辉锑矿、白钨矿、黄铁矿和粉砂质粘土条带（粉砂级石英＋绢云母＋绿泥石）构成（图3b）。这种韵律层在厚度仅数十厘米的矿层内可达十几至数十个，韵律层理与矿层和围岩的层理一致。厘米级至毫米级厚的单个条带或纹层，在走向及倾向方向上常可追溯数米至上百米远。局部地段，矿层与围岩同步揉皱；但在另一些情况下，矿层发生揉皱而其上下围岩却未变形（图3c）。值得一提的是，在层状矿体附近的顶底板（尤其是底板）围岩中，见有数层整合产出的无矿石英和碳酸盐〔铁白云石＋方解石（白云石）〕。这些无矿的石英-碳酸盐层厚度仅为数毫米至数厘米，但顺层可追溯至数百米远，其内部常发育许多不对称的、多数轴面倾向北西的小揉皱，但紧邻其上下的围岩却无变形现象，层理平直、清晰，这是一种典型的软变形构造（图2、图3d）。

脉状-网脉状矿化占总储量的25%强，产于层状矿体下盘3～10 m范围内的板岩中（图2、图3e）。矿化以数十至上百条与层状矿体高角度相交和少数近于平行的白钨矿-含金石英细脉为特征，细脉带形态呈透镜状或楔状，一般走向长20～60 m，倾向延深40～120 m。单条细脉呈平整的板状，厚0.5～5 cm，延伸1～5 m，脉间距5～50 cm。

除上述两种主要的矿化外，局部偶见沿裂隙或节理充填的石英±白钨矿±辉锑矿±碳酸盐脉，主要发育于层状矿体发生揉皱的核部地带并常切穿层状矿体（图2、图3f），表明其形成与变形期间的再活化作用有关。

作为重要找矿标志的围岩蚀变，在层状矿体的上下盘呈基本整合的层状产出，厚0.2～2 m，局部可达10 m（图2、图3a）。通常，下盘蚀变的强度和厚度略大于上盘，蚀变带与围岩之间为渐变过渡关系。与未蚀变的紫红色板岩相比，蚀变岩石呈黄白色、灰白色或浅肉红色，因而也被称为褪色化蚀变。蚀变矿物呈弥散状或斑点状，局部沿微裂隙充填产出，矿物组合包括石英、绢云母、绿泥石、黄铁矿和碳酸盐（铁白云石±白云石），有时含少量浸染状电气石和重晶石。蚀变带岩石保留了清晰的层理构造。

2　矿物学和组构学特征

在沃溪矿床，矿石的矿物组合较为简单。金属矿物主要有辉锑矿、白钨矿、黄铁矿和自然金，其次为毒砂、黑钨矿、闪锌矿、方铅矿，微量矿物包括黝铜矿、黄铜矿、车轮矿、块硫锑铅矿、辉砷镍矿和方锑金矿。脉石矿物以石英占绝对优势，次为方解石、白云石、铁白云石、菱铁矿、绢云母、绿泥石、重晶石、电气石、磷灰石等。次生矿物包括针铁矿、纤铁矿、锑华、方锑矿、黄锑矿、孔雀石、蓝铜矿、铜蓝等，仅偶见于矿体上部的局部地段。下面将简要描述若干主要矿物的形貌和组构特征。
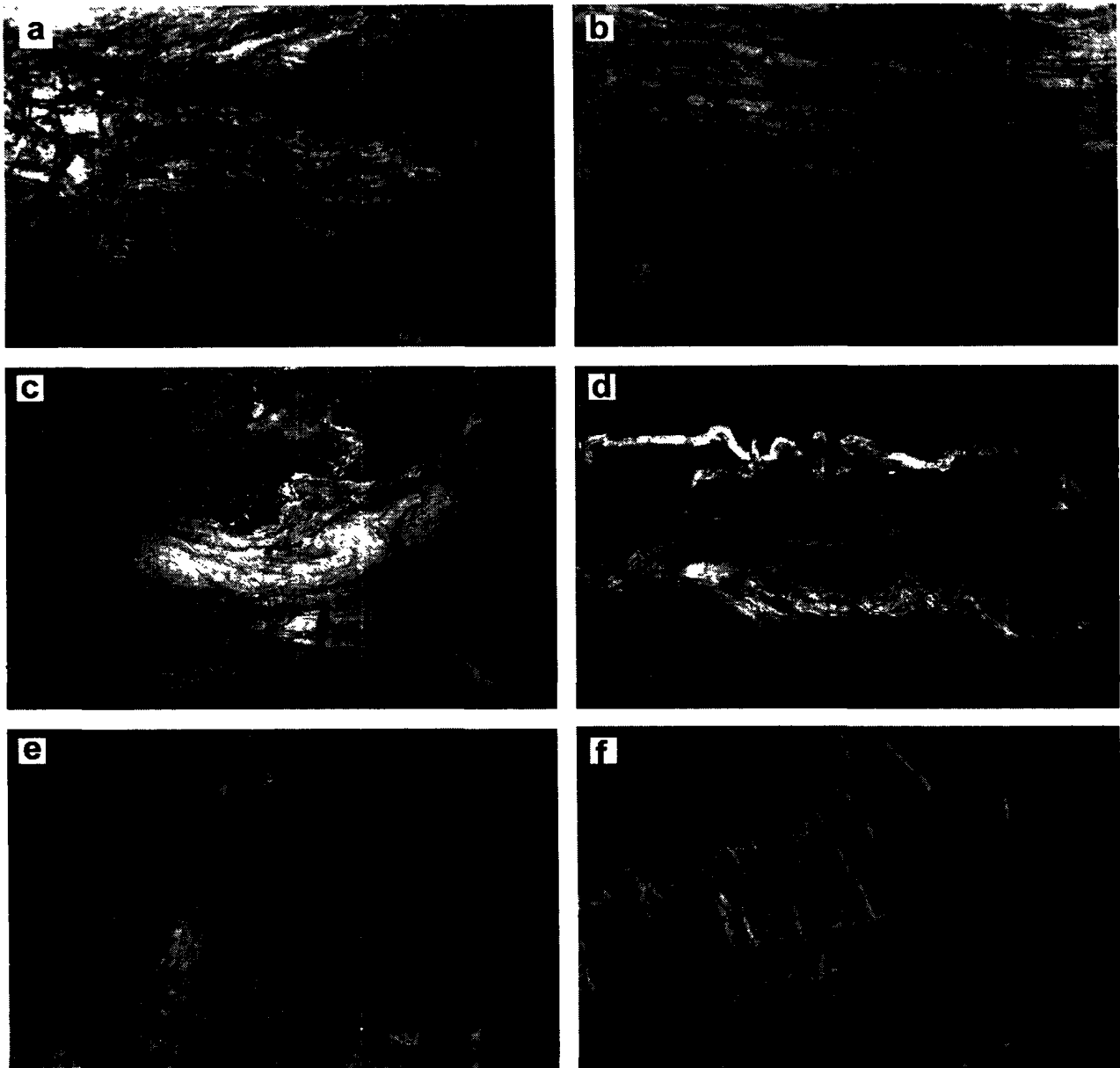
2.1　辉锑矿

作为沃溪矿床中含量最丰富的一种硫化物，辉

图 3 沃溪矿床中两种主要矿化类型的宏观特征

a—层状矿体及其两侧围岩的褪色化蚀变；b—层状矿体局部放大，矿石由条带状/层纹状辉锑矿（黑色）、石英＋白钨矿（白色）和粉砂质粘土条带（灰色）的韵律互层组成；c—条带状/层纹状矿石发生揉皱，但下盘围岩层理平坦、未变形；d—近矿体蚀变围岩中顺层产出的无矿石英-碳酸盐（白色），内部发育不对称的、多数轴面倾向一致的小揉皱（软变形构造）；e—层状矿体下盘与地层高角度相交的脉状矿化；f—局部沿裂隙或节理发育的石英-白钨矿细脉切割层纹状矿石

Fig. 3 Macroscopic features of two main mineralization types in the Woxi deposit

a—Stratiform ores and associated "bleached" alteration; b—Typical and close views of stratiform ores: banded to finely laminated stibnite (black), quartz + scheelite (white), and silty clays (gray); c—Stratiform ores illustrating soft-sediment deformation. Note the relatively undeformed footwall and hanging-wall metasediments; d—Asymmetric, small-scale folds of barren quartz-carbonate layers (white) bounded above and below by undisturbed metasediments, indicating soft-sediment deformation; e—Quartz-scheelite stringer veins and veinlets subvertical to overlying stratiform ores; f—Locally observed discordant and cleavage-filling veinlets of scheelite-quartz crosscutting stratiform and laminated scheelite-quartz ore

锑矿在层状矿石中呈毫米级至分米级厚的细纹层状、条带状或块状产出，并与含金石英、白钨矿、黄铁矿和粉砂质粘土构成韵律互层(图3a、3b、3c)。在显微镜下，辉锑矿条带和(或)纹层由等粒至不等粒、极细粒($5\mu m$)至粗粒(可达6 mm)的晶体集合体构成(图4a、4b、4c)。通常，单一纹层的晶体粒度大致相等，多数为10 μm左右。在细粒辉锑矿集合体中，有时可见到由拟态结晶作用形成的辉锑矿的他形变斑晶(>0.5 mm,图4c)，且变斑晶中常可识别出残余的作为其前身的辉锑矿微晶。有时，辉锑矿集合体中含有大量的石英、绢云母、黄铁矿等显微包裹物，这些包裹物呈与层理和(或)纹层平行的定向排列(图4b)。这是一种典型的"内沉积组构"——si组构(Sander,1970)，代表了原始沉积层理的残余(讨论见后)。在宏观至微观尺度上，辉锑矿条带或纹层常与共生的含金石英、白钨矿、黄铁矿纹层和粘土条带同步揉皱、碎裂甚至局部糜棱岩化。结晶后的晶格变形常导致压力双晶的出现和辉锑矿晶体的波状消光等(图4d、4e)。

辉锑矿是沃溪矿床中的重要载金矿物之一，含金量(w_{Au})可达110 $\times 10^{-6}$(罗献林等,1996)。金在辉锑矿中主要呈次显微-超显微形式出现，部分呈显微金产出(Gu et al.,2002b)。.

2.2　白钨矿

白钨矿主要在层状矿体中呈条带状、层纹状、壳层状、透镜状产出，其次在细脉矿化带中呈石英-白钨矿-黄铁矿脉、网脉产出(图3)。白钨矿晶体粒度变化大(从小于0.02 mm到大于20 mm)，多为他形的粒状或板状，极少数为半自形晶。他形板状的大晶体通常破碎并大致沿ss(∥s)面定向排列，破碎后的白钨矿多被石英、铁白云石、方解石、黄铁矿等矿物胶结(图4f)。有时可见白钨矿的示顶底组构和软变形构造(图4g、图5a)。与辉锑矿相似，白钨矿有时也具si组构，晶体内平行层理和(或)纹理排列的固体显微包裹体主要为石英和绢云母，次为黄铁矿、重晶石、磷灰石、毒砂和辉锑矿。

在紫外光照射下，层状和脉状矿石中的白钨矿均发浅兰色荧光(图5b)，反映两者具相似的化学组分。电子探针分析表明，两种产状的白钨矿在常量和微量元素组成上无明显区别，且均不含金(Gu et al.,2002b)。

2.3　黄铁矿

黄铁矿具多种形态和较大的粒度变化范围(从1

μm至8 mm)。按粒度、形态和产出特征的不同，主要可分为3类：①极细粒($<5\mu m$)的浑圆状、变胶状或不规则状黄铁矿，它们集中沿层理和/或纹理呈毫米级厚的微层产出(图5c、5d)；②顺层产出的中至粗粒，常具环带且富含包裹物的立方体晶或自形变晶黄铁矿(图5e、5f)；③石英-碳酸盐-黄铁矿细脉，其中的黄铁矿多沿脉壁生长，通常为细至中粒，自形或半自形，部分具环带，清洁无包裹物(图5g)。

上述的中至粗粒且通常具环带的立方体或自形变晶黄铁矿，往往显示出精美的si组构，其中的大量石英、绢云母、黝铜矿等微米级固体包裹物多呈大致平行于外部层理或纹理的方向定向排列(图5f)。有时，这种黄铁矿的自形变晶由一个富含包裹物的内核和一个无包裹物的清洁的均质外环构成。后期变形作用常使黄铁矿自形变晶碎裂并被石英、碳酸盐、辉锑矿、白钨矿等矿物胶结。

电子探针分析表明，上述3类黄铁矿在Fe,S,As,Au等元素含量上无显著差别。在总计90个分析点中，67个点(约占75%)探测到含量高于检出限的金(w_{Au}一般在0.01% ~0.48%之间；Gu et al.,2002b)。同一个颗粒中不同分析点的金含量变化很大，表明其中的金可能主要以次显微-超显微的包裹体形式出现。

2.4　自然金

可见金(包括明金和显微金)在沃溪矿床中约占金总量的20%(罗献林等,1996)，它们多呈他形粒状或不规则状包裹于石英、辉锑矿和黄铁矿中(图5h、5i)，有时呈细脉状产于上述矿物的微裂隙中。自然金粒度变化大(从小于1 μm到数毫米)，杂质含量低，成色高(958~993,Gu et al.,2002b)。

2.5　石英

石英是本矿床中占绝对优势的非金属矿物，主要在层状矿体中呈块状、条带状、层纹状产出，其次在细脉矿化带中呈脉状、网脉状产出(图3)。粒度最细的他形粒状石英微晶(2~8 μm)集合体呈单矿物纹层产出(图5j)，可能代表了矿床中最早的矿物世代。多期的重结晶和(或)增生结晶作用(也称聚粒结晶作用)，使层纹状微晶石英的粒度显著增大(可达10 mm左右)。有时，富含流体和固体(绢云母)包裹体的早期石英被后期重结晶的无包裹物的清洁石英所增生。同结晶期至结晶期后的构造变形，常影响到几乎所有粒级的石英颗粒，导致碎裂结构、波状消光、∥s面理的定向拉长(图5k)、"错动"构造
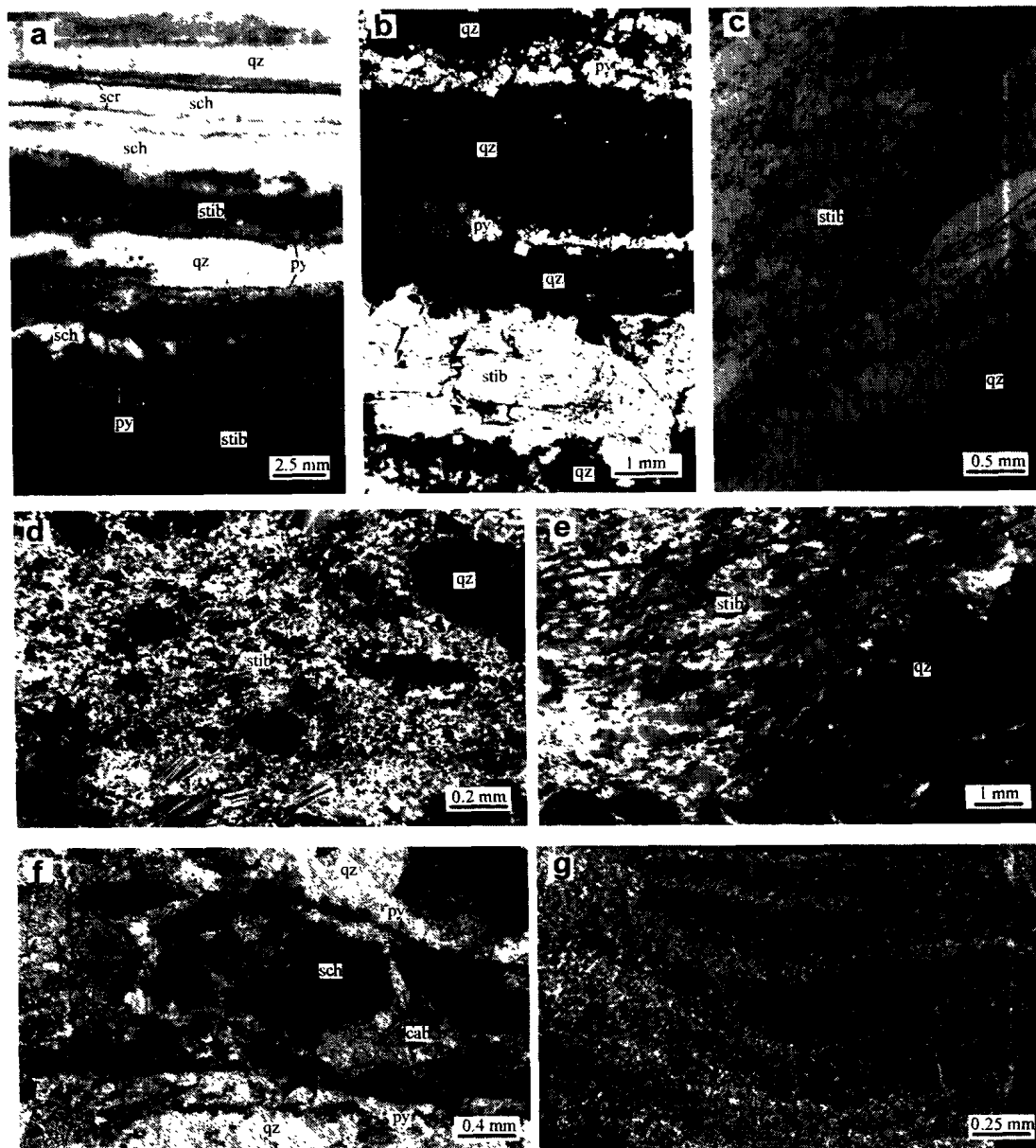
图 4　典型矿石组构的显微照片

a—由辉锑矿、黄铁矿、白钨矿、石英和绢云母构成的显微层纹状构造,各纹层间的界线清晰、整合,光片,斜交偏光; b—石英、辉锑矿和黄铁矿的互层构成显微层纹状构造,他形辉锑矿变斑晶中含大量平行层理方向排列的显微固体包裹体(石英＋绢云母,黑色斑点),光片,单偏光; c—由辉锑矿粒度和形态变化显示的显微纹理与颗粒拉伸所显示的片理化方向一致(左下—右上对角方向),光片,斜交偏光; d—细粒辉锑矿集合体及其中具双晶结构的辉锑矿他形变晶,光片,斜交偏光; e—构造变形引起的辉锑矿晶体的定向拉伸、波状消光以及围绕刚性石英颗粒的绕曲现象,光片,斜交偏光; f—被黄铁矿和石英纹层所围限的板状白钨矿晶体破碎并为碳酸盐胶结,薄片,单偏光; g—白钨矿的示顶底构造,槽形层理的凹面指示顶面,薄片,正交偏光。矿物代号: cab—碳酸盐; py—黄铁矿; qz—石英; sch—白钨矿; ser—绢云母; stib—辉锑矿

Fig. 4　Photomicrographs of typical ore fabrics at Woxi

a—Fine layering of stibnite, pyrite, scheelite, quartz and sericite. Note the sharp and conformable boundaries between different microlayers. Polished section, nicols ×; b—Micro-layering of quartz, stibnite and pyrite. Note the s-oriented microinclusions (black, predominantly quartz and sericite) in stibnite xenoblasts. Polished section. 1 nicol; c—Fine lamination shown by change in grain size and form of stibnite crystallites parallel to the schistosity (left bottom to right top) illustrated by elongation of stibnite grains. Polished section, nicols ×; d—Twinning stibnite xenoblasts in fine-grained stibnite aggregate. Polished section, nicols ×; e—Elongation, undulating extinction and curving of ductile stibnite crystallites around rigid quartz aggregates caused by tectonic deformation. Polished section, nicols ×; f—Tabular scheelite crystals bounded by pyrite and quartz microlayers are fractured and cemented by carbonate. Thin section, 1 nicol; g—Geopetal scheelite texture in calcareous slate, with concave indicating upper surface. Thin section, nicols +. Abbreviat: cab—Carbonate; py—Pyrite; qz—Quartz; sch—Scheelite; ser—Sericite; stib—Stibnite
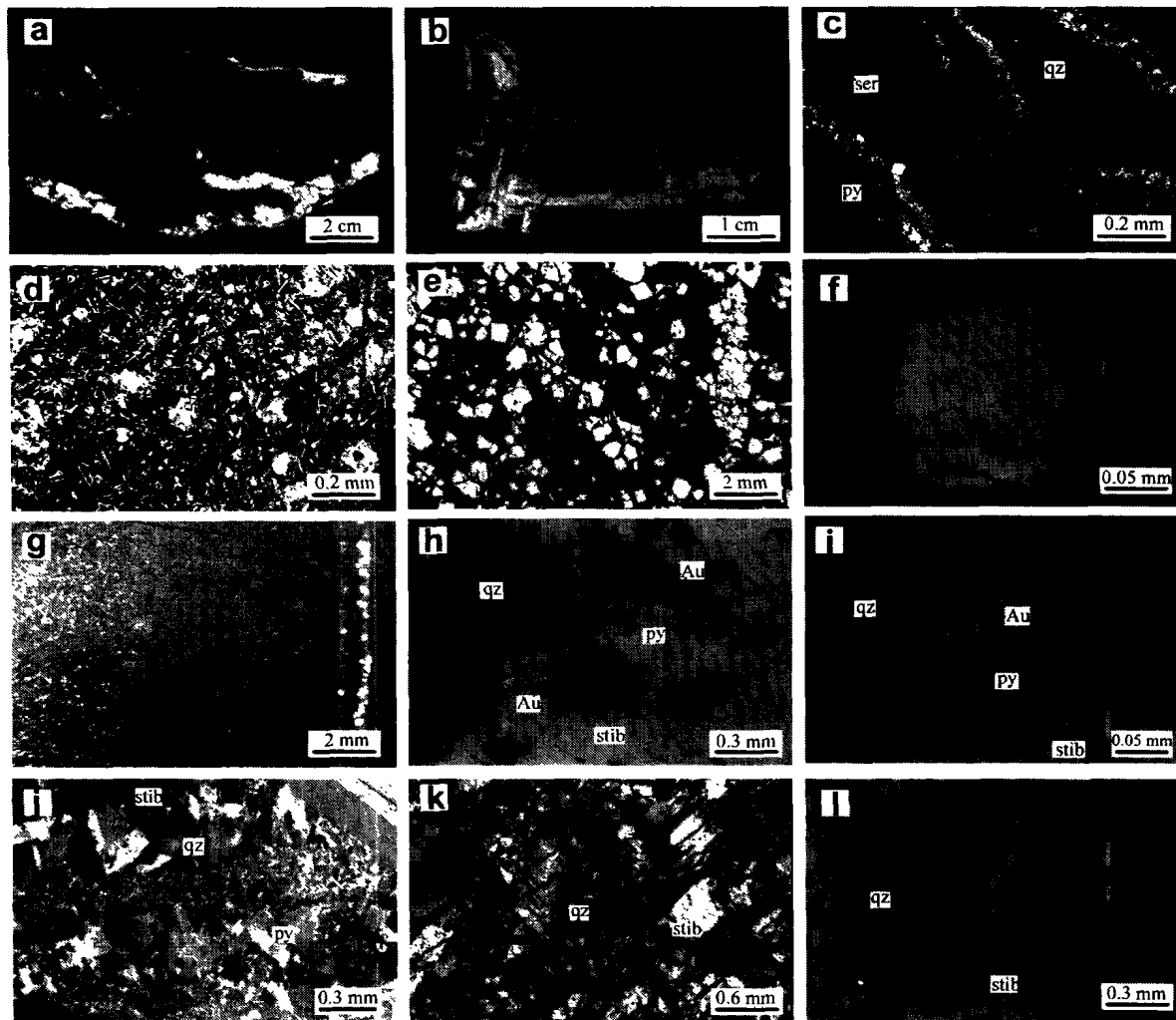
图 5 沃溪矿床的典型矿石组构

a—条带状白钨矿（白色）-辉锑矿（灰黑色）-石英（灰色）矿石的软变形构造,手标本,紫外光下； b—石英-白钨矿脉切割层纹状白钨矿,手标本,紫外光下； c—由极细粒的黄铁矿集合体和石英、绢云母构成的显微层纹状构造,纹层局部变形弯曲,光片,单偏光； d—层状矿石中的浑圆状、变胶状、不规则状黄铁矿,左下—右上的对角线为层理方向,光片,单偏光； e—层状矿石中的中至粗晶自形黄铁矿,左上—右下的对角线为层理方向,光片,单偏光； f—内核富含显微固体包裹体（石英＋绢云母＋金红石,黑色斑点）的黄铁矿被一个无包裹物的均质外环增生,包裹物大致沿平行外部层理（水平）的方向排列（si 组构）,光片,单偏光； g—含浸染状黄铁矿的蚀变板岩被一石英-黄铁矿-碳酸盐细脉切割,光片,单偏光； h—辉锑矿中的显微自然金（Au）,光片,单偏光； i—黄铁矿中的显微包裹金（Au）,光片,单偏光； j—由不同粒级的石英和黄铁矿构成的显微层纹状构造,辉锑矿沿裂隙产出、薄片,斜交偏光； k—辉锑矿沿石英集合体的两组裂隙产出,其中的一组（左下—右上对角）与层理方向一致,石英具定向拉长和波状消光现象,薄片,斜交偏光； l—各种形态和粒级的碎裂状石英为辉锑矿胶结,光片,单偏光。矿物代号同图 4

Fig. 5 Typical ore fabrics of the Woxi deposits

a—Soft-sediment deformation of banded scheelite (white)-stibnite(gray black)-quartz (gray) ore. Hand specimen under short wave UV-light; b—Quartz-scheelite veins/veinlets crosscutting laminated scheelite. Hand specimen under short wave UV-light; c—Partly folded, micro-layering of very fine-grained pyrite, quartz and sericite. Polished section, 1 nicol; d—Subrounded to irregular, crustiform pyrite. Bedding: diagonal (left bottom to right top). Polished section, 1 nicol; e—Median- to coarse-grained, euhedral pyrite disseminates in stratiform ores. Bedding: diagonal (left top to right bottom). Polished section, 1 nicol; f—A pyrite idioblast comprises an inclusion-rich core overgrown by an inclusion-free, homogeneous rim. The microinclusions (black spots) consist of sericite, quartz, and rutile and are oriented roughly parallel to external bedding/lamination of host rocks and ores (si fabric). Polished section, 1 nicol; g—A discordant quartz-pyrite-carbonate veinlet in altered slate with pyrite disseminates. Polished section, 1 nicol; h—Native gold (Au) in stibnite. Polished section, 1 nicol; i—Native gold (Au) locked in pyrite euhedra. Polished section, 1 nicol; j—Fine laminations shown by different grain sizes of quartz and pyrite. Stibnite occurs as fissure-fillings. Thin section, nicols ×; k—Stibnite infilled along two sets of microfissures in quartz aggregate, one of which (left bottom to right top) corresponds to the primary bedding of the sediments. Note also the elongation and undulating extinction of quartz aggregate. Thin section, nicols ×; l—Cataclastic quartz with different forms and grain sizes cemented by stibnite. Thin section, 1 nicol. Abbretives of minerals as for Fig. 4

（图 51,讨论见下）以及石英纹层的褶皱等现象的发育。

石英也是沃溪矿床中的重要载金矿物之一（Gu et al., 2002b）。罗献林等（1996）报道,石英中的金含量可达 151×10^{-6}。

3 讨 论

海底喷流作用对成矿的意义以及同生热水沉积学说,现已得到矿床学家的普遍认同,这在很大程度上是由于大量现代海底正在活动的热液喷流成矿系统的发现以及对与此相对应的各类古代多金属矿床研究资料的丰富积累（Bonatti, 1975; Hekinian et al., 1980; Cann et al., 1982; Robbins, 1983; Rona et al., 1983; 1993; Rona, 1984; 1989; Roberts, 1997; Lüders et al., 2001）。一般认为,火山喷流作用主要与贱金属块状硫化物矿床的形成有关,并通常伴生有典型的诸如 Fe-Si 质化学沉积物、重晶石岩、电气石岩、毒重岩、Fe-Mg 氧化物等喷流岩（Large et al., 1989; Leblanc et al., 1990; Cas, 1992; Large, 1992; Robinson et al., 1996; Sherlock et al., 1999; Doyle et al., 1999）,而非火山的沉积喷流过程则被认为可能与多种类型矿床的形成有关,包括产于沉积岩中的 SEDEX 型 Pb-Zn-Ag 多金属矿床（Hamilton et al., 1982; Strens et al., 1987; Goodfellow et al., 1993; Sewell et al., 1994; Whitehead et al., 1996; Fernandez et al., 1997; Large et al., 1998; Sangster et al., 1998; Paradis et al., 1998; Cooke et al., 2000）、镜铁矿矿床（薛春纪等, 1997）、重晶石矿床（Clark et al., 1991; MacIntyre, 1992）、Ni-Mo 多金属矿床（Lott et al., 1999）、Sn-多金属矿床（韩发等,1989a;1989b; 1990; 1997; Jiang et al., 1999）以及部分微细浸染型金矿床（Zheng et al., 1993; Gu, 1996; 顾雪祥等, 2000; Emsbo et al., 1999; Gu et al., 1996; 2002d）等。本文所研究的沃溪矿床,代表了沉积喷流型矿床谱系中的另一重要成员。

3.1 矿床同生成因的组构学证据

无论在宏观还是微观尺度上,沃溪矿床中层状矿化的最为显著的特征都是频繁的由硫化物、白钨矿、含金石英和粉砂质粘土构成的韵律互层和精美的条带状、层纹状构造（图 2、图 3a-d、图 3f、图 4a-c）,正如在许多沉积喷流（SEDEX）型矿床中所见到的那样（韩发等, 1989a; 1997; Large et al., 1998; Paradis et al., 1998; Jiang et al., 1998; 1999; Emsbo et al., 1999）。在局部地段,层状矿体及其中的条带和纹层与其所赋存的浅变质沉积岩同步揉皱,表明矿化发生于区域变质-变形作用之前。另一方面,条带状矿石中以及层状矿体附近无矿的石英-碳酸盐层中常见的由构造滑塌和重力滑移所形成的软变形构造（图 3c、图 3d、图 5a）,指示了矿化发生于浊积岩形成的同时。

层状矿体中毫米级至厘米级厚的辉锑矿、白钨矿、黄铁矿、含金石英等化学沉积物的条带或纹层与陆源的粉砂质粘土条带呈频繁的韵律互层产出,条带或纹层的产状与围岩的层理一致,并在走向及倾向方向上可追溯数米至上百米远。各条带或纹层之间在微观尺度上的界线清晰且整合（图 4a、4b）,如此清晰、整合的接触界线用后生充填-交代的假说是难以令人信服的（Large et al., 1998）。Cooke 等（参见 Large et al., 1998）的化学模拟表明,倘若条带状/层纹状构造由充填-交代作用形成,则会出现复杂的脉石矿物侧向分带现象。然而,这种分带现象在沃溪矿床中却未曾见及。

尽管沃溪矿床中的多数黄铁矿在成岩及变质作用期间发生了重结晶,但极细粒（$1 \sim 5\mu m$）的浑圆状、变胶状或不规则状的黄铁矿在层纹状矿石中仍得以很好的保存（图 5c、5d）。变胶状结构,也被称为球状、葡萄状-肾状或网状结构（Foley et al., 2001）,是海相和陆相喷流型矿床中常见的一种典型结构（Eldridge et al., 1983; Large, 1992; Poulsen et al., 1996; Gu, 1996; Foley et al., 2001）。通常认为,这种结构要么是在由含矿热流体与海水混合而导致的快速冷却状态下的亚稳定胶体溶液中形成的,要么是在矿石沉淀过程中通过硫化物原地交代细菌或生物残留体而生成的。这两种方式都可能适合于解释本矿床中细粒变胶状黄铁矿的形成机理,但从变胶状、浑圆状黄铁矿总是与针状、不规则状黄铁矿共生（图 5d）的特点来看,后一种方式,即硫化物原地交代细菌或生物残留体（藻类?）的可能性更大。在沃溪矿床中,具上述结构的黄铁矿在含粉砂和粘土的黄铁矿纹层中较在黄铁矿的单矿物纹层中更为丰富,表明它们在变质和构造变形中受到了周围稳定物质的保护。Ramdohr（1980）指出,通过细菌作用形成的细粒硫化物球体具有抗重结晶作用的能力,因而在某些情况下,它们往往是受变质的岩石或矿石中

唯一得以保留下来的残存结构。

中至粗粒的立方体晶或自形变晶黄铁矿，通常含大量的大致沿平行于外部层理或纹理方向定向排列的微米级固体包裹体（图5f）。一般认为，这种"内沉积组构"（si组构）系先存的黄铁矿微细球粒在增生结晶或聚粒结晶为粗大晶体过程中，原微细球粒间的沉积物被圈闭所形成的。这些被圈闭的陆源碎屑矿物的排列仍保留了原始沉积层理的方向，因此，这种组构被认为是同沉积成因的可靠证据（Sander，1970；Zheng et al.，1993；Gu，1996；Gu et al.，2002d）。有时，富含固体包裹体的黄铁矿被一个无包裹物的均质外环所增生，后者可能形成于区域变质作用过程。

白钨矿和辉锑矿均属极易重结晶为粗大晶体的矿物，因而它们的原始组构特征通常易于被掩盖或破坏。然而，在沃溪矿床的层状矿石中却仍然保留了丰富的指示同沉积成因的组构学证据，如白钨矿的示顶底和软变形构造（图4g、图5a）、辉锑矿-白钨矿-石英显微层纹状构造（图4a～c、图5b）、白钨矿和辉锑矿的si组构（图4b）等。

矿床同生成因的进一步证据，包括层状矿体与脉状-网脉状矿体之间的相互关系以及蚀变带的空间产出特征等。如前所述，沃溪矿床中的脉状-网脉状矿化仅出现于层状矿体下盘3～10 m范围内的蚀变板岩中（图2，图3e），表明这些矿化的细脉很可能代表了沉积喷流系统中的矿液补给带。鉴于矿床中未能识别出形成层状矿体的持续、聚流排泄的通道系统（如同沉积断裂），因而推测矿液并非集中排泄到某一特定的沉积场所，而是沿海水底界以下未石化的沉积物柱中弥散的、与裂隙有关的网状通道向上排泄到海底的。矿床中典型的两组（与层状矿体高角度相交的和近平行的）矿化细脉，彼此相互贯通，脉体具开放裂隙空间充填的特征，表明通道系统的矿液压力可能接近于，并间歇性地高于静岩压力；而且，水力压裂型的网状通道系统可能发育于接近海水/沉积物界面的张应力区域（Large，1992）。

沃溪矿床中，层状矿体下盘围岩蚀变的强度和厚度均大于上盘蚀变，这与在许多后生的、热液充填-交代型矿床中所见到的现象有着明显的区别，后者的上盘围岩通常比下盘遭受更为强烈和更为广泛（厚）的蚀变作用，尤其是当成矿过程中矿脉的产状平缓时更为如此（Dubé et al.，1998）。笔者认为，沃溪矿床中整合产出的层状蚀变体与矿化体一样，也

是同生沉积作用的产物。下盘和上盘的蚀变带以及共生的无矿石英-碳酸盐层，分别代表了成矿之前和成矿之后海底热液活动早期和晚期的产物；下盘的蚀变在矿液沿弥散的网状通道向上排泄过程中得以进一步增强和加厚。

细脉状矿化位于层状矿化之下以及下盘蚀变强度和厚度大于上盘，是喷流型矿床中的两种常见现象（Gemmell et al.，1992；Whitehead et al.，1996；Robinson et al.，1996；Sherlock et al.，1999；Doyle et al.，1999）。笔者认为，同生沉积成因的观点最能合理地解释上述层状矿体、细脉状矿化以及围岩蚀变之间的空间关系。矿化的多层位现象表明，成矿是幕式的，并周期性地发生浊流沉积作用。每一期喷流以化学和机械的混合沉积为序幕（下盘蚀变带），以含矿热卤水的大量排泄为高潮（层状矿化，以化学沉积为主夹有极少量的远洋粉砂质粘土），最终又以化学和机械的混合沉积为帷幕（上盘蚀变带）。

3.2 沉积后变质-变形的组构学证据

宏观尺度上，变质-变形作用对沃溪矿床的影响包括：①局部地段矿层与围岩的同步揉皱；②主要沿平行层理/纹理方向的剪切；③矿质的再活化以及局部切层的后期裂隙脉的形成。

微观尺度上，变质作用使几乎所有的矿石矿物和脉石矿物都因重结晶而粒度加大。另一方面，由于不同矿物流变特性的差异，变质-变形的结果导致若干脆性或韧性微组构的形成。黄铁矿、毒砂、石英、白钨矿等相对刚性的矿物主要显示碎裂结构（图4f、图5k），而塑性的辉锑矿则围绕刚性组分弯曲或拉长（图4e）。有时，棱角状至浑圆状的各种形态与大小的刚性石英碎块同时被塑性的辉锑矿基质所胶结（图5l），指示了一种次生构造成因的所谓"错动构造"（Marshall et al.，1989）。辉锑矿和碳酸盐矿物的压力双晶、波状消光、∥s面理的定向拉长等现象常见，指示了剪切、位错、晶格变形等作用的存在。在细粒辉锑矿集合体中见到的辉锑矿他形变斑晶多呈定向伸长，边界不规则（图4c），这归因于以成核和颗粒边界位移为主要标志的动力重结晶作用（Pesquera et al.，1993）。

4 结　论

沃溪矿床代表了沉积喷流型（SEDEX）矿床谱系中的一个新的重要成员。指示矿床同生成因的组构

学证据主要有：① 硫化物、白钨矿、含金石英以及远洋沉积物(粉砂质粘土)的频繁韵律互层和精美的条带状、层纹状构造；② 整合的层状矿体与围岩的同步揉皱；③ 由构造滑塌和重力滑移引起的软变形构造；④ 细粒黄铁矿的变胶状结构；⑤ 黄铁矿、辉锑矿、白钨矿等矿物中丰富的 si 组构等。与许多火山或沉积喷流型矿床中类似的层状矿体、细脉状矿化以及围岩蚀变之间的空间关系，指示了矿石与其所赋存的围岩同时形成。矿床形成后的变质-变形作用，尽管使多数矿物发生了重结晶、碎裂、位错乃至小范围的再活化等，但却并未改变矿化的整体特征和矿床的工业利用价值。

海水通过在沉积柱中的循环萃取矿质，并进而沿弥散的、与裂隙有关的网状通道向上排泄到海底，通过化学沉积作用而成矿。成矿作用是幕式的，并周期性地发生浊流沉积作用，这便导致了矿化体在赋矿层序中的多次重复出现。每一期喷流作用都以化学和机械的混合沉积为序幕，以含矿热卤水的大量排泄为高潮，最终又以化学和机械的混合沉积为帷幕。

References

Bao Z X. 1989. Stratabound antimony deposits in western Hunan [J]. Mineral Deposits, 8 (4): 49 ~ 60 (in Chinese with English abstract).

Bao Z X. 1990. Minerogenetic-geological features and exploratory indicators of gold in W-Sb-As-Au ore deposits of West Hunan Province [J]. Mineral Resources and Geology, 4 (3): 18 ~ 25 (in Chinese with English abstract).

Bao Z X and He G X. 1991. Geologic and geochemical features of Woxi W-Sb-Au ore deposit in western Hunan [J]. Hunan Geology, 10 (3): 207 ~ 216 (in Chinese with English abstract).

Bonatti E. 1975. Metallogenesis at oceanic spreading centers [J]. Annual Review of Earth and Planetary Science, 3: 401 ~ 431.

Cann J R and Strens M R. 1982. Black smokers and freezing magma [J]. Nature, 298: 147 ~ 149.

Cas R A F. 1992. Submarine volcanism: Eruption styles, products, and relevance to understanding the host-rock successions to volcanic-hosted massive sulfide deposits [J]. Econ. Geol., 87: 511 ~ 541.

Clark S H B and Orris G J. 1991. Descriptive model of exhalative barite [A]. In: Orris G J and Bliss J D, ed. Some industrial mineral deposit models: descriptive deposit models [C]. U. S. Geological Survey, Open File Report. 21 ~ 22.

Cooke D R, Bull S W, Large R R, et al. 2000. The importance of oxidized brines for the formation of Australian Proterozoic stratiform sediment-hosted Pb-Zn (sedex) deposits [J]. Econ. Geol., 95: 1 ~ 17.

Doyle M G and Huston D L. 1999. The subsea-floor replacement origin of the Ordovician Highway-Reward volcanic-associated massive sulfide deposit, Mount Windsor Subprovince, Australia [J]. Econ. Geol., 94: 825 ~ 844.

Dubé B, Dunning G and Lauzière K. 1998. Geology of the Hope Brook Mine, Newfoundland, Canada: A preserved late Proterozoic high-sulfidation epithermal gold deposit and its implications for exploration [J]. Econ. Geol., 93: 405 ~ 436.

Eldridge C S, Barton P B Jr and Ohmoto H. 1983. Mineral textures and their bearing on formation of the Kuroko orebodies [J]. Econ. Geol., (Monograph 5): 241 ~ 281.

Emsbo P, Hutchinson R W, Hofstra A H, et al. 1999. Syngenetic Au on the Carlin trend: Implications for Carlin type deposits [J]. Geol., 27: 59 ~ 62.

Fernandez M J and Velasco F. 1997. The Troya Zn-Pb carbonate-hosted SEDEX deposit, northern Spain [A]. In: Sangster D F, ed. Carbonate-hosted lead-zinc deposits [C]. Society of Economic Geologists, Special Publication 4. 364 ~ 377.

Foley N, Ayuso R A and Seal R. 2001. Remnant colloform pyrite at the Haile gold deposit, South Carolina: A textural key to genesis [J]. Econ. Geol., 96: 891 ~ 902.

Gemmell J B and Large R R. 1992. Stringer system and alteration zones underlying the Hellyer volcanic-hosted massive sulfide deposit, Tasmania, Australia [J]. Econ. Geol., 87: 620 ~ 649.

Goodfellow W D, Lydon J W and Turner R J W. 1993. Geology and genesis of stratiform sediment-hosted (SEDEX) zinc-lead-silver sulphide deposits [A]. In: Kirkham R V, Sinclair W D, Thorpe R I, et al., ed. Mineral deposit modeling [C]. Geological Association of Canada, Special Paper 40. 201 ~ 251.

Gu X X. 1996. Turbidite-hosted micro-disseminated gold deposits [M]. Chengdu: Chengdu University of Science and Technology Press. 1 ~ 239.

Gu X X, Schulz O and Vavtar F. 1996. Unusual relict fabrics of realgar in the sediment-hosted disseminated gold deposits in NW-Sichuan, China: evidence for syngenetic origin with epigenetic remobilization [A]. International Geological Congress abstracts, volume 2 of 3 [C]. 1996-8-4 ~ 14. Beijing. 777.

Gu X X, He B B, Schulz O, et al. 2000. Relict sedimentary fine-laminated fabrics of stibnite and its genetic significance in the Manaoke stratabound gold deposit, Sichuan, China [J]. J. Chengdu Univ. Techn., 27(4): 331 ~ 334 (in Chinese with English abstract).

Gu X X, Liu J M, Zheng M H, et al. 2002a. Provenance and tectonic setting of the Proterozoic turbidites in Hunan, South China: Geo-

chemical evidence [J]. J. Sedimentary Research, 72 (3): 393~407.

Gu X X, Schulz O, Vavtar F, et al. 2002b. Jung-proterozoische submarine Primäranreicherung und metamorphogene Weiterentwicklung der stratiformen W-Sb-Au-Erzlagerstätten vom "Typ Woxi" in Hunan (Süd-China) [M]. Vienna: Archiv für Lagerstätten der Geologische Bundersanstalt 23. 1~204.

Gu X X, Schulz O, Vavtar F, et al. 2002c. Rare earth element geochemical constraints on the genesis of the Woxi W-Sb-Au deposit, South China [J]. Geochim. Cosmochim. Acta, 66 (Supp. 1): A295.

Gu X X, Liu J M, Schulz O, et al. 2002d. Syngenetic origin for the sediment-hosted disseminated gold deposits in NW-Sichuan, China: Ore fabric evidence [J]. Ore Geol. Rev., 22: 91~116.

Hamilton J M, Bishop D T, Morris H C, et al. 1982. Geology of the Sullivan orebody, Kimberly, B.C., Canada [A]. In: Hutchinson R W, Spence C D and Franklin J M, ed. Precambrian sulfide deposits, H S Robinson Memorial Volume [C]. Geological Association of Canada Special Paper 25. 597~666.

Han F and Hutchinson R W. 1989a. Evidence for exhalative origin for rocks and ores of the Dachang tin-polymetallic field: the ore-bearing formation and hydrothermal exhalative sedimentary rocks [J]. Mineral Deposits, 8 (2): 25~40 (in Chinese with English abstract).

Han F and Hutchinson R W. 1989b. Evidence for hydrothermal exhalative sedimentary origin of the Dachang tin-polymetallic deposits——geochemistry of rare earth elements and trace elements of the host rocks [J]. Mineral Deposits, 8 (3): 33~42 (in Chinese with English abstract).

Han F and Hutchinson R W. 1990. Evidence for exhalative origin of the Dachang tin-polymetallic sulfide deposits: Their geological and geochemical characteristics [J]. Mineral Deposits, 9 (4): 309~324 (in Chinese with English abstract).

Han F, Zhao R S, Shen J Z, et al. 1997. Geology and genesis of the Dachang tin-polymetallic deposits [M]. Beijing: Geol. Pub. House. 1~213 (in Chinese with English abstract).

Hekinian R, Fevrier M, Bischoff J L, et al. 1980. Sulphide deposits from the East Pacific Rise, near 21°N [J]. Science, 207: 1433~1444.

Jiang S Y, Palmer M R, Slack J F, et al. 1998. Paragenesis and chemistry of multistage tourmaline formation in the Sullivan Pb-Zn-Ag deposit, British Columbia [J]. Econ. Geol., 93: 47~67.

Jiang S Y, Han F, Shen J Z, et al. 1999. Chemical and Rb-Sr, Sm-Nd isotopic systematics of tourmaline from the Dachang Sn-polymetallic ore deposit, Guangxi Province, P. R. China [J]. Chem. Geol., 157: 49~67.

Large R R, Huston D L, McGoldrick P J, et al. 1989. Gold distribution and genesis in Australian volcanogenic massive sulfide deposits, and their significance for gold transport models [J]. Econ. Geol., (Monograph 6): 520~536.

Large R R. 1992. Australian volcanic-hosted massive sulfide deposits: Features, styles, and genetic models [J]. Econ. Geol., 87: 471~510.

Large R R, Bull S W, Cooke D R, et al. 1998. A genetic model for the HYC deposit, Australia: Based on regional sedimentology, geochemistry, and sulfide-sediment relationship [J]. Econ. Geol., 93: 1345~1368.

Leblanc M and Billaud P. 1990. Zoned and recurrent deposition of Na-Mg-Fe-Si exhalites and Cu-Fe sulfides along synsedimentary faults (Bleïda, Morocco) [J]. Econ. Geol., 85: 1759~1769.

Li J Y. 1989. Geological features of the Woxi Au-Sb-W ore deposit [J]. Geology and Exploration, 25 (12): 1~7 (in Chinese with English abstract).

Liang J C, Shi J, Yi S J, et al. 1981. A preliminary discussion on micro-textures and fabrics of quartz layers in the Woxi gold deposits in Hunan [J]. Bulletin of Guilin College of Metallurgical Geology, 1 (3): 41~52 (in Chinese with English abstract).

Liang Y B and Zhang Z R. 1986. Typomorphic characteristics of quartz from the Woxi Au-Sb-W deposit, western Hunan [J]. Hunan Geol., 5 (2): 17~24 (in Chinese).

Liang Y B and Zhang Z R. 1988. A geneto-mineralogical study of main minerals from the Woxi Au-Sb-W deposit, western Hunan [J]. Geology and Exploration, 24 (8): 25~30 (in Chinese with English abstract).

Liu Y J. 1992a. Study on the ore-controlling fault structure in the Woxi gold deposit [J]. Mineral Resources and Geology, 6 (1): 29~34 (in Chinese).

Liu Y J. 1992b. Fold structure of the Woxi gold-antimony-tungsten deposit in western Hunan and its ore-controlling regularity as well as dynamic ore-forming process [J]. Mineral Deposits, 11 (2): 134~141 (in Chinese with English abstract).

Liu Y J. 1993. Study on dynamic ore-forming processes of fault structures in Woxi gold deposit, Hunan [J]. J. Chengdu College of Geo-logy, 20 (1): 50~55 (in Chinese with English abstract).

Liu Y J, Sun C Y and Ma D S. 1993. Jiangnan-type gold deposits and their ore-forming geochemical background [M]. Nanjing: Nanjing Univ. Press. 1~260 (in Chinese).

Lott D A, Coveney R M Jr, Murowchick J B, et al. 1999. Sedimentary exhalative nickel-molybdenum ores in South China [J]. Econ. Geol., 94: 1051~1066.

Lüders V, Pracejus B and Halbach P. 2001. Fluid inclusion and sulfur isotope studies in probable modern analogue Kuroko-type ores from the JADE hydrothermal field (Central Okinawa Trough, Japan) [J]. Chem. Geol., 173: 45~58.

Luo X L, Yi S J and Liang J C. 1984. On the genesis of the Woxi Au-Sb-W deposit, W-Hunan [J]. Geology and Exploration, 20 (7): 1~10 (in Chinese).

Luo X L, Zhong D Q, Li G S, et al. 1996. Geology of the Woxi-type stratabound gold deposits in Hunan Province [M]. Beijing: Seismic Press. 1~313 (in Chinese).

MacIntyre D G. 1992. Geological setting and genesis of sedimentary exhalative barite and barite-sulfide deposits, Gataga District, northeastern British Columbia [A]. In: Jonasson I R, ed. Exploration

and Mining Geology 1[C]. International Association on the Genesis of Ore Deposits, Eighth Quadrennial Symposium. 1~20.

Mao J W and Li H Y. 1997. Research on genesis of the gold deposits in the Jiangnan terrain [J]. Geochemistry, 26 (5): 71 ~ 81 (in Chinese with English abstract).

Marshall B and Gilligan L B. 1989. Durchbewegung structure, piercement cusps, and piercement veins in massive sulfide deposits: Formation and interpretation [J]. Econ. Geol., 84: 2311~2319.

Meng X M and Xie J R. 1965. Classification and metallogenesis of ore deposits [M]. Beijing: Sci. Press (in Chinese).

Niu H C and Ma D S. 1992. Metallogenesis of stratabound gold deposits in western Hunan [J]. Mineral Deposits, 11 (1): 65 ~ 75 (in Chinese with English abstract).

Paradis S, Nelson J L and Irwin S E B. 1998. Age constraints on the Devonian shale-hosted Zn-Pb-Ba deposits, Gataga district, Northeastern British Columbia, Canada [J]. Econ. Geol., 93: 184 ~ 200.

Peng B. 1992. A preliminary study on the fault tectonic-metallogenetic mechanism of the Woxi gold mine, W-Hunan [J]. Geotectonica et Metallogenia, 16 (2): 176~177 (in Chinese).

Pesquera A and Velasco F. 1993. Ore metamorphism in sulfide mineralization from the Cinco Villas Massif (Western Pyrenees, Spain) [J]. Econ. Geol., 88: 266~282.

Poulsen K H and Hannington M D. 1996. Volcanic-associated massive sulfide gold [M]. Geological Survey of Canada. 183 ~ 196.

Ramdohr P. 1980. The ore minerals and their intergrowths (Volume 2) [M]. 2nd ed. Oxford: Pergamon Press. 1~1205.

Robbins E I. 1983. Accumulation of fossil fuels and metallic minerals in active and ancient rift lakes [J]. Tectonophysics, 94: 633~658.

Roberts H H. 1997. Evidence of episodic fluid, gas, and sedimentary venting on the Northern Gulf of Mexico continental slope [J]. Econ. Geol., 92: 863~879.

Robinson M, Godwin C I and Stanley C R. 1996. Geology, lithogeochemistry, and alteration of the Battle volcanogenic massive sulfide zone, Buttle Lake Mining Camp, Vancouver Island, British Columbia [J]. Econ. Geol., 91: 527~548.

Rona P A, Bostroim K and Smith K L Jr. 1983. Hydrothermal processes at seafloor spreading centers [M]. New York: Plenum Press. 1~796.

Rona P A. 1984. Hydrothermal mineralization at seafloor spreading centers [J]. Earth-Science Reviews, 20: 1~104.

Rona P A. 1989. Hydrothermal mineralization at oceanic ridge [J]. Canadian Mineralogist, 26: 431~465.

Rona P A and Scott S P. 1993. A special issue on sea-floor hydrothermal mineralization: New perspective—Preface [J]. Econ. Geol., 88: 1933~1976.

Sander B. 1970. An introduction to the study of fabrics of geological bodies [M]. Braunschweig: Pergamon Press. 1~641.

Sangster D F and Hillary E M. 1998. Sedex lead-zinc deposits: proposed sub-types and their characteristics [J]. Exploration and Mining Geology, 7: 341~357.

Schulz O, Vavtar F, Gu X X, et al. 2001. Submarin-hydrothermale Metallanreicherung im Jung-Proterozoikum und Metamorphogene Weiterentwicklung der stratiformen W-Sb-Au-Erzlagerstätten vom "Typ Woxi" in Hunan, Südost-China. Mitt [J]. österr. Miner. Ges., 146: 263~265.

Sewell D M and Wheatley C J V. 1994. The Lerokis and Kali Kuning submarine exhalative gold-silver-barite deposits, Wetar Island, Maluku, Indonesia [J]. J. Geochemical Exploration, 50: 351 ~ 370.

Sherlock R L, Roth T, Spooner E T C, et al. 1999. Origin of the Eskay Creek precious metal-rich volcanogenic massive sulfide deposit: Fluid inclusion and stable isotope evidence [J]. Econ. Geol., 94: 803~824.

Strens M R, Cann D L and Cann J R. 1987. A thermal balance model of the formation of sedimentary-exhalative lead-zinc deposits [J]. Econ. Geol., 82: 1192~1203.

Tu G C, et al. 1984. Geochemistry of Chinese stratabound ore deposits (Volume 1) [M]. Beijing: Sci. Press. 189~218 (in Chinese).

Tu G C, et al. 1987. Geochemistry of Chinese stratabound ore deposits (Volume 2) [M]. Beijing: Sci. Press. 1~299 (in Chinese).

Whitehead R E, Davies J F, Valdes-Nodarse E L, et al. 1996. Mineralogical and chemical variations, Castellanos shale-hosted Zn-Pb-Ba deposit, Northwestern Cuba [J]. Econ. Geol., 91: 713~722.

Xiao Q M and Li D K. 1984. Discussion on the genesis of antimony deposits in Hunan [J]. Mineral Deposits, 11 (3): 13 ~ 24 (in Chinese with English abstract).

Xu K Q. 1965. Genesis of ore deposits [M]. Beijing: Geol. Pub. House(in Chinese).

Xue C J, Ji J S, Zhang L C, et al. 1997. The Jingtieshan submarine exhalative-sedimentary iron-copper deposit in North Qilian Mountain [J]. Mineral Deposits, 16 (1): 21 ~ 30 (in Chinese with English abstract).

Yang X. 1992. Source of ore material and paragenesis of ore building elements in Woxi Au-Sb-W deposit, Hunan [J]. J. Chengdu College of Geology, 19 (2): 20 ~ 28 (in Chinese with English abstract).

Zhang L G. 1985. Stable isotope geology of the tungsten-antimony-gold deposits in the Xuefeng Uplift region, West Hunan [J]. Geology and Exploration, 21 (11): 24~28 (in Chinese).

Zhang L G. 1995. Studies on isotopic geochemistry in China [M]. Beijing: Sci. Press. 241~266 (in Chinese).

Zhang Z R. 1980. The genesis and ore-forming mechanism of the Woxi Au-Sb-W deposit, Taoyuan [J]. Science Information of the Metallurgical Institute of South China, 1~10 (in Chinese).

Zhang Z R. 1989. Research on gold deposits [M]. Changsha: Press of China Industrial University. 1~190 p (in Chinese).

Zheng M H, Liu J M, Schulz O, et al. 1993. Schichtgebundene Goldlagerstätten in kambrischen und triassischen Gesteinen in NW-Sichuan (China) [M]. Archiv für Lagerstätten der Geologische Bundesanstalt, Band 15. 1~152.

Zhu Y L, Li C R and Lin Y Z. 1981. Geology of tungsten deposits in

South China [M]. Nanchang: Jiangxi People's Pub. House (in Chinese).

附中文参考文献

鲍振襄. 1989. 湘西西部层控锑矿床[J]. 矿床地质, 8 (4)：49~60.

鲍振襄. 1990. 湘西钨锑砷金矿床中金的成矿地质特征与找矿标志[J]. 矿产与地质, 4 (3)：18~25.

鲍振襄, 何谷先. 1991. 湘西沃溪钨锑金矿床地质地球化学特征[J]. 湖南地质, 10 (3)：207~216.

顾雪祥, 何彬彬, Schulz O, 等. 2000. 四川马脑壳层控金矿床中辉锑矿残余沉积组构的发现及其成因意义[J]. 成都理工学院学报, 27 (4)：331~334.

韩　发, 哈钦森 R. W. 1989a. 大厂锡-多金属矿床热液喷气沉积成因的证据：含矿建造及热液沉积岩[J]. 矿床地质, 8 (2)：25~40.

韩　发, 哈钦森 R. W. 1989b. 大厂锡-多金属矿床热液喷气沉积成因的证据：容矿岩石的微量元素及稀土元素地球化学[J]. 矿床地质, 8 (3)：33~42.

韩　发, 哈钦森 R. W. 1990. 大厂锡-多金属矿床喷气沉积成因的证据：矿床地质和地球化学特征[J]. 矿床地质, 9 (4)：309~324.

韩　发, 赵汝松, 沈建忠, 等. 1997. 大厂锡多金属矿床地质及成因[M]. 北京：地质出版社. 1~213.

李键炎. 1989. 沃溪金锑钨矿床的地质特征[J]. 地质与勘探, 25 (12)：1~7.

梁金城, 石　锦, 易诗军, 等. 1981. 湘西沃溪金矿床层状石英脉的显微构造与组构探讨[J]. 桂林冶金地质学院学报, 1 (3)：41~52.

梁博益, 张振儒. 1986. 湘西沃溪金锑钨矿床石英的标型特征研究[J]. 湖南地质, 5 (2)：17~24.

梁博益, 张振儒. 1988. 湘西沃溪金锑钨矿床成因矿物学研究[J]. 地质与勘探, 24 (8)：25~30.

刘亚军. 1992a. 沃溪金矿床断裂构造控矿的研究[J]. 矿产与地质, 6 (1)：29~34.

刘亚军. 1992b. 湘西沃溪金锑钨矿床褶皱构造及其控矿规律与动力

成矿作用[J]. 矿床地质, 11 (2)：134~141.

刘亚军. 1993. 湖南沃溪金矿断裂构造动力成矿研究[J]. 成都地质学院学报, 20 (1)：50~55.

刘英俊, 孙承辕, 马东升. 1993. 江南金矿及其成矿地球化学背景[M]. 南京：南京大学出版社. 1~260.

罗献林, 易诗军, 梁金城. 1984. 论湘西沃溪金锑钨矿床的成因[J]. 地质与勘探, 20 (7)：1~10.

罗献林, 钟东球, 李高生, 等. 1996. 湖南省沃溪式层控金矿地质[M]. 北京：地震出版社. 1~313.

毛景文, 李红艳. 1997. 江南古陆某些金矿床成因讨论[J]. 地球化学, 26 (5)：71~81.

孟宪民, 谢家荣. 1965. 矿床分类与成矿作用[M]. 北京：科学出版社.

牛贺才, 马东升. 1992. 湘西层控金矿床成因机制的研究[J]. 矿床地质, 11 (1)：65~75.

彭　渤. 1992. 湘西沃溪金矿田断层构造成矿机理初探[J]. 大地构造与成矿学, 16 (2)：176~177.

涂光炽, 等. 1984. 中国层控矿床地球化学（第一卷）[M]. 北京：科学出版社. 189~218.

涂光炽, 等. 1987. 中国层控矿床地球化学（第二卷）[M]. 北京：科学出版社. 1~299.

肖启明, 李典奎. 1984. 湖南锑矿成因探讨[J]. 矿床地质, 3 (3)：13~24.

徐克勤. 1965. 矿床成因论[M]. 北京：地质出版社.

薛春纪, 姬金生, 张连昌, 等. 1997. 北祁连镜铁山海底喷流沉积铁铜矿床[J]. 矿床地质, 16 (1)：21~30.

杨　燮. 1992. 湖南沃溪金锑钨矿床成矿物质来源及成矿元素的共生机制[J]. 成都地质学院学报, 19 (2)：20~28.

张理刚. 1985. 湘西雪峰山隆起区钨锑金矿床稳定同位素地质学[J]. 地质与勘探, 21 (11)：24~28.

张理刚. 1995. 中国同位素地球化学研究[M]. 北京：科学出版社. 241~266.

张振儒. 1980. 桃源沃溪金锑钨矿床成因及成矿机理研究[J]. 中南矿冶学院科技情报, 1~10.

张振儒. 1989. 金矿研究[M]. 长沙：中南工业大学出版社. 1~190.

朱炎龄, 李崇偌, 林运淮. 1981. 华南钨矿地质[M]. 南昌：江西人民出版社.

Ore Fabric Characteristics of Woxi W-Sb-Au Deposit in Hunan and Their Genetic Significance

Gu Xuexiang[1], Oskar Schulz[2], Franz Vavtar[2], Liu Jianming[3] and Zheng Minghua[4]

(1 Institute of Geochemistry, Chinese Academy of Sciences, Guiyang 550002, Guizhou, China; 2 Institute of Mineralogy and Petrography, University of Innsbruck, A-6020 Innsbruck, Austria; 3 Institute of Geology and Geophysics, Chinese Academy of Sciences, Beijing 100101, China; 4 Chengdu University of Technology, Chengdu 610059, Sichuan, China)

Abstract

Ore fabric studies of the Woxi W-Sb-Au deposit on macro- to micro- scales have revealed that the deposit is

of syngenetic hydrothermal sedimentary origin. Ore fabric evidence for a syngenetic origin mainly includes: (1) rhythmical, fine layering/banding of sulfides, scheelite, quartz, and pelagic metasediments, (2) folding of both ore layers and their host rocks, (3) soft-sediment deformation due to slumping and synsedimentay sliding, (4) colloform textures of fine-grained pyrite, and (5) abundant si fabrics in minerals of pyrite, stibnite and scheelite. The intimate spatial relationships between the stratiform ores, the stringer veins, and the alteration blankets suggest coeval deposition of the ores and their host metasediments. Postdepositional metamorphism and tectonic deformation chiefly resulted in recrystallization, cataclasm, dislocation, and small-scale remobilization of minerals.

Key words: geology, ore fabrics, sedimentary exhalation, syngenetic origin, W-Sb-Au deposit, Woxi, Hunan Province

Intergrowth of Wolframoixiolite and W-rich Manganocolumbite in Dajishan Tungsten Deposit, Jiangxi Province, South China

Zhang Wenlan, Hua Renmin and Wang Rucheng

(Key State Laboratory for Mineral deposits Research, Nanjing University, Nanjing 210093, Jiangsu, China)

Abstract

The Dajishan tungsten deposit in Jiangxi Province is of quartz-wolframite-vein type. The mineralized granite is an Early Yanshanian granitic complex, which consists from old to young of medium-megagrained porphyroid biotite monozonitic granite, medium-grained muscovite alkali-feldspar granite and Nb-, Ta-rich fine-grained rare element muscovite granite (69# body).

The Dajishan tungsten deposit is associated mainly with the second stage medium-to-fine grained two-mica granite. Some aggregates of Nb(Ta)-Mn(Fe)-W complex oxides were found in fractures along the borders of wolframite or scheelite. Back-scattered electron images show that the aggregates consist of two components whose brightness is different from each other. The darker one is columbite, whereas the brighter one is considered to be wolframoixiolite, a complex Nb(Ta)-Mn(Fe)-W oxide mineral. The wolframoixiolite is intimately intergrown with manganocolumbite, and changes gradually in composition into W-rich manganocolumbite. Considering their modes of occurrence and EPMA data, it is held that the intergrown W-rich manganocolumbite and wolframoixiolite are related to the third stage Nb-Ta-rich fine-grained granite. The granite was enriched in Nb-Ta-rich fluids at the late evolution stage, and such a type of fluid must have replaced the early-formed wolframite, leading to successive crystallization of wolframoixiolite and W-rich manganocolumbite. All this suggests that there probably exist a wide replacement range between wolframite and columbite in the nature.

Key words: mineralogy, W-rich manganocolumbite, wolframoixiolite, isomorphic replacement, Dajishan tungsten deposit